Structural Evaluation of Cell-filled Pavements Using Finite Element Model

Subrat Roy

Indian Institute of Science Education and Research,Bhopal, Madhya Pradesh, India

Abstract—**This paper presents the performance evaluation of cell-filled pavements using finite element model. The model of the pavement structure was developed using *ANSYS*, finite element software [1]. The concept of cell-filled pavement was developed in South Africa [2], [3]. Cell-filled pavement consists of laying a formwork of cells of plastic sheet over a compacted sub-base. The cells as are stretched along the carriageway and tensioned by using steel pegs. Cement bound materials are filled into the cells and compacted. During compaction, cell walls get deformed and provide interlocking among the blocks. Thus, the load carrying capacity of the surface layer is mainly dependent on the interlocking property of the blocks which, in turn, is governed by the degree of deformation of the plastic wall during construction. Interlocking among the cells of the cell-filled layer has been modeled using surface contact elements. Using the finite element model, Structural performance was evaluated in terms of surface deflections and vertical sub grade strains on top of the sub grade.**

Keywords— **Finite Element Model, Cell Fill Pavement**

I. INTRODUCTION

The pavement has been modeled as a three layer system consisting of cell-filled layer, subbase and subgrade. Typical section considered for analysis is shown in Figures 1(a) and 1(b). The size of the pavement considered is 2400 mm × 2400 mm. Depth of subgrade layer has been taken as 2000 mm. Cell-filled layer was represented by the size of the cell, layer thickness and the elastic modulus and Poisson's ratio of the material used in the layer. Subbase layer and subgrade are represented by their thickness, elastic moduli and Poisson's ratio values. Interface contact elements were used to model the cell layer / subbase and subbase / subgrade interface.

The size of the cell was considered as 150 mm × 150 mm. Considering the symmetry about X-axis and Y-axis (in figure 5.1b), a quarter model was adopted as shown in Figure 2. For convenience, a square load contact area of 300 mm × 300 mm was considered.
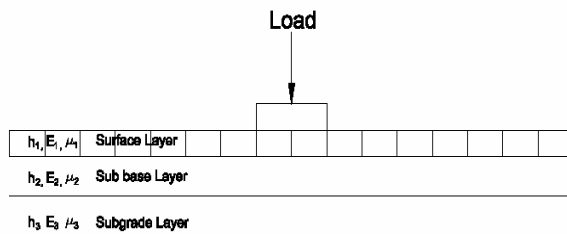

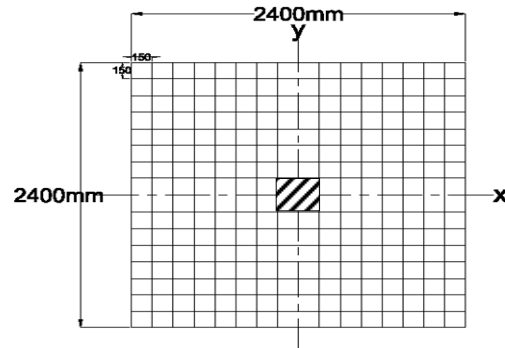Fig. 1(a) A typical three-layer pavement system
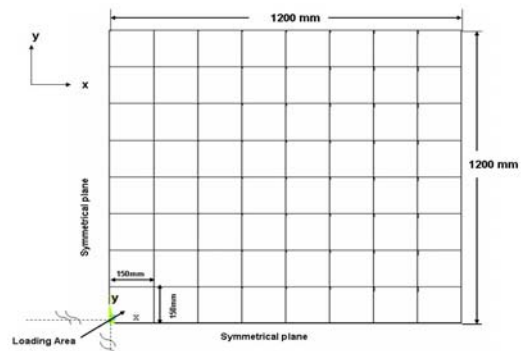

Fig. 1(b) Pavement model dimensions in plan

Fig. 2 Top view of quarter model

II. ELEMENTS USED IN MODELING

The three layers of the pavement were discretized using 8-noded solid elements (SOLID45). The element is defined by 8 nodes having three degrees of freedom at each node, translations in nodal x, y, and z directions at each node. Figure 3 shows the SOLID45 geometry (source: ANSYS).
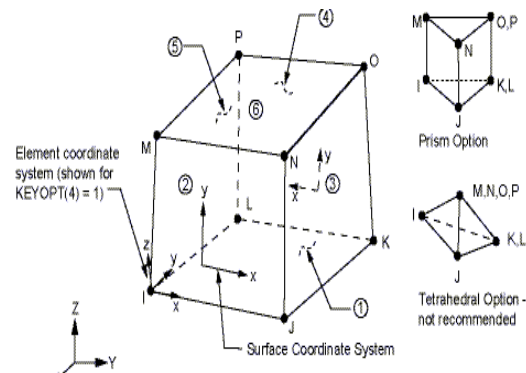

Fig. 3 SOLID 45Geometry (source: ANSYS)

A. Contact element (surface- to- surface contact element)

The surface-to-surface contact elements were used to simulate the interlocking or friction between the cells. Surface-to-surface contact element can be used to model either rigid -

flexible or flexible- flexible contact between surfaces. It involves a contact between two boundaries. One of the boundaries is conventionally established as the "target" surface and other as the "contact" surface. These two surfaces together comprise the "contact pair". In the present investigation, 3-D contact pairs, TARGET 170 with CONTACT 173, were used.

B. CONTACT 173 Geometry

CONTACT 173 element, shown in Figure 4, was used to represent contact and sliding between 3-D "target" surfaces (TARGET170) and a deformable surface. This element is applicable to 3-D structural and coupled field contact analysis. It has the same geometrics as the SOLID 45 element face with which it is connected. Contact occurs when the element surface penetrates one of the target segment elements on a specified target surface. Coulomb and shear stress friction can be simulated. The element is defined by 4 nodes.

The node ordering is consistent with the node ordering for the underlying solid element. The positive normal is given by the right-hand rule going around the nodes of the element and is identical to the external normal direction of the underlying solid element surface. The nodal ordering between solid and contact element defines bottom surface contact.
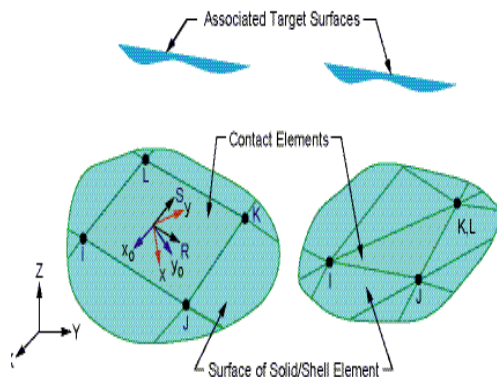

Fig. 4 CONTACT 173 Elements (source: ANSYS)

C. TARGET 170 geometry

Target-170 element (4 node quadrilateral), shown in Figure 5, is used to represent various 3-D "target" surfaces for associated contact elements. This target surface is discretized by a set of target segment elements (TARGET170) and is paired with its associated contact surface via a shared real constant set. It can impose any translational or rotational displacement. It can also impose forces and moments on target elements.
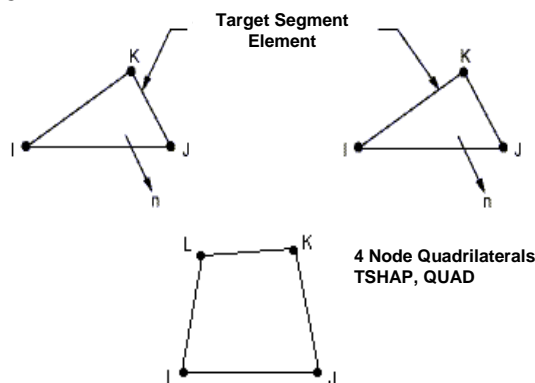

Fig. 5 TARGET 170 Elements (source ANSYS)

III. MESHING

The research carried out by Hjelmstad et al. [4] concluded that the element shape can significantly control the model analysis in terms of its run-time and accuracy. Cunagin and Grubbs [5] illustrated that critical stresses and peak deflection occur around the wheel loads and decrease in the far-field. In the study proposed by Zaghloul and white [6], fine meshes were used under the wheel path. Figures 6 and 7 show a representative 3D finite element mesh of a cell-filled pavement system. Considering the symmetry about X-axis and Y-axis, quarter model was considered. The dimensions of the elements are not uniform as shown in the figures. Elements are smaller in size nearer to the wheel loads where stress and deflection gradient are steeper. This justifies the need for fine mesh around loading area. The boundary conditions applied are:

(i)   Along the axis of symmetry:
      $U_y = 0$ in X – direction and $U_x = 0$ in Y – direction.
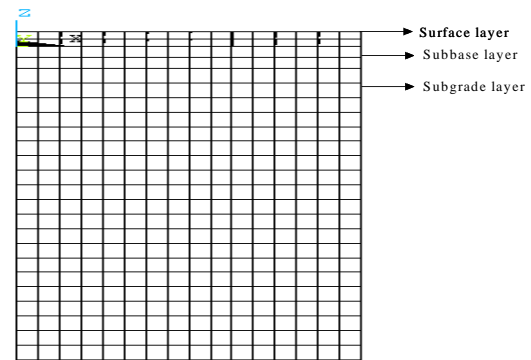(ii)   At the bottom of the subgrade all the degrees of freedom are constrained.
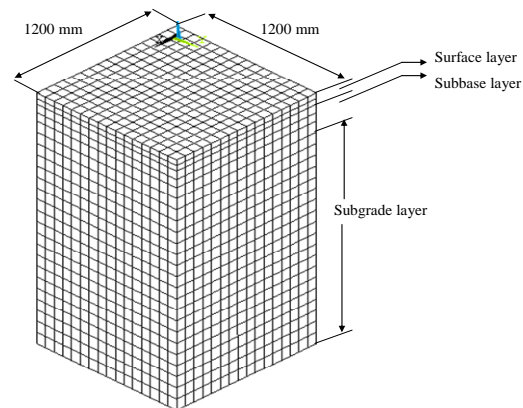

Fig. 6 Elevation of finite element mesh

Fig. 7 3D Finite element mesh of pavement

IV. EFFECT OF LAYER MODULI ON THE BEHAVIOR OF CELL-FILLED PAVEMENT

The finite element pavement model, developed in the present study was used to carryout sensitivity analysis for evaluation of influence of layer moduli on the structural behaviour of cell-filled pavement. Structural behaviour was evaluated in terms of surface deflection and vertical subgrade strain.

A. Effect of subbase layer modulus on the structural behaviour of cell-filled pavement

Material properties considered for sensitivity analysis to find out the effect of subbase layer modulus on the structural behaviour of cell-filled pavement, are given below. While the modulus of subbase material was varied, properties of other materials were kept constant.

- Elastic moduli of cell-filled material – 31000 MPa,
- Elastic modulus of subbase material – 50 MPa, 100 MPa, 150 MPa, 200 MPa, 250 MPa and 300 MPa.
- Elastic modulus of subgrade – 80 MPa
- Coefficient of friction between the cell-filled concrete blocks – 0.6.

The model was subjected to a pressure of 0.58 MPa. Results are presented in Tables 1 and 2 and also in Figures 8 and 9.

TABLE I- Effect of subbase modulus on surface deflection

Subbase material stiffness (MPa)	Deflection (mm) obtained at load center
50	0.6057
100	0.5618
150	0.5277
200	0.4998
250	0.4774
300	0.459

TABLE II- Effect of subbase modulus on vertical subgrade strain

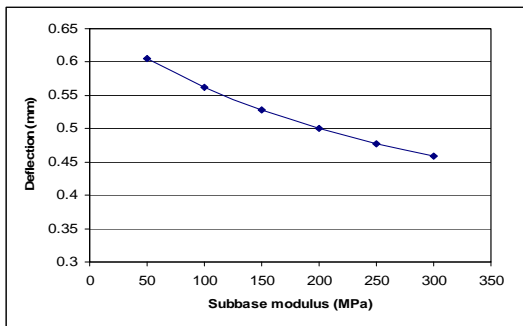| Subbase material stiffness (MPa)	Vertical subgrade strain × 10^{-4}
50	9.87
100	7.91
150	6.71
200	5.92
250	5.35
300	4.92

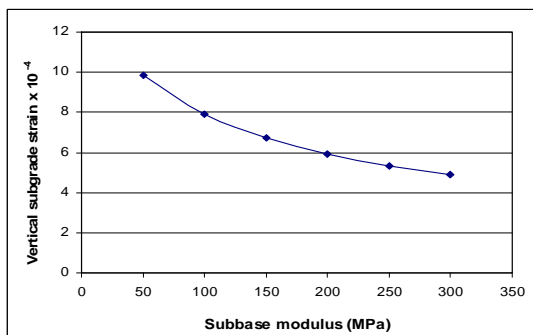Fig. 8 Effect of subbase modulus on surface deflection

Fig. 9 Effect of subbase modulus on vertical subgrade strain

B. Effect of subgrade modulus on the structural behaviour of cell-filled pavement

Material properties considered for sensitivity analysis to find out the effect of subgrade modulus on the structural behavior of cell-filled pavement, are given below. While the modulus of subgrade was varied, properties of other materials were kept constant.

- Elastic moduli of cell-filled material – 31000 MPa,
- Elastic modulus of subbase material – 150 MPa.
- Elastic moduli of subgrade – 10 MPa, 20 MPa, 30 MPa, 40 MPa, 50 MPa, 60 MPa, 70 MPa, 80 MPa, 90 MPa and 100 MPa.
- Coefficient of friction between the cell-filled blocks – 0.6.

The model was subjected to a pressure of 0.58 MPa. Results are presented in Table 3 and also in Figure 10.

TABLE III
Effect of subgrade modulus on surface deflection

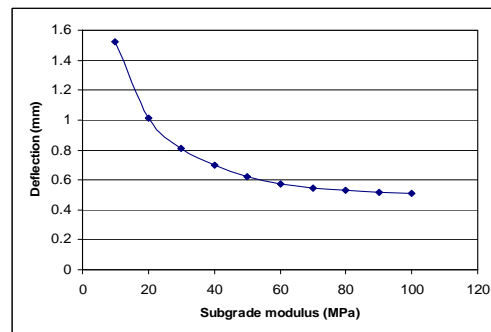| Subgrade stiffness (MPa)	Deflection (mm) obtained at load center
10	1.52
20	1.011
30	0.8126
40	0.6999
50	0.6249
60	0.5704
70	0.5432
80	0.5277
90	0.5181
100	0.5113

Fig. 10 Effect of subgrade modulus on surface deflection

V. CONCLUSION

From the sensitivity analysis, it is observed that the load spreading ability of a cell-filled pavement is substantially dependent on the stability of its subbase layer and subgrade. The layer modulus increases the stability of a pavement by influencing surface deflection and vertical subgrade strain. By increasing the elastic modulus value of subbase layer from 50 MPa to 300 MPa, the pavement surface deflection decreased by 24% where as the vertical subgrade strain reduced by 50%. By increasing the elastic modulus value of subgrade from 10 MPa to 100 MPa, the pavement surface deflection decreased by 66%. The stiffness of the subgrade has a much greater influence on the surface deflection than the subbase stiffness. As the subgrade modulus value falls below 20 MPa, the maximum deflection of the pavement surface increases rapidly.

Similarly, the subbase modulus has greater influence on the vertical subgrade strain than on the surface deflection. As the subbase modulus value falls below 100 MPa, the vertical subgrade strain increases rapidly.

REFERENCES

[1]. ANSYS Users' Manual, ANSYS Inc., Canonsburg, PA, 2002.

[2]. Visser, T. A. and Hall, S. (1999). "Flexible Portland Cement Concrete Pavement for Village Roads", Transportation Research Record 1652, Transportation Research Board, Washington D.C., pp. 121-127

[3]. Visser, T. A. and Hall, S. (2003). "Innovative and Cost Effective Solutions for Roads in Rural Areas and difficult terrain", Transportation Research Record: Journal of Transportation Research Board, Volume 1819A/2003, pp. 169-173.

[4]. Hjelmstad, K. D., Kim, J. and Zuo, Q. H. (1997). "Finite Element Procedures for Three-dimensional Pavement Analysis," Aircraft Pavement/Technology – In the midst of Change, ASCE, Seattle, WA, USA, pp. 125-137.

[5]. Cunagin, W. D. and Grubbs, A. B., (1991). "Automated Acquisition of Truck Tyre Pressure Data," Transportation Research Record 1322, TRB, National Research Council, Washington D.C., pp. 112-121.

[6]. Zaghloul, S., and White, T. (1992). "Use of Three-Dimensional Dynamic Finite Element Program for Analysis of Flexible Pavement," Transportation Research Record 1388, Transportation Research Board, Washington D.C., pp. 60-69.